Non-Coherent Massive MIMO Systems: A Constellation Design Approach

Xie, H., Xu, W., Ngo, H-Q., & Li, B. (2020). Non-Coherent Massive MIMO Systems: A Constellation Design Approach. *IEEE Transactions on Wireless Communications*, *19*(6), 3812 - 3825. https://doi.org/10.1109/TWC.2020.2978806

Published in:
IEEE Transactions on Wireless Communications

Document Version:
Peer reviewed version

Non-coherent Massive MIMO Systems: A Constellation Design Approach

Huiqiang Xie, Weiyang Xu, *Member, IEEE*, Hien Quoc Ngo, *Member, IEEE*, Bing Li

Abstract

In this paper, a joint multi-user constellation is proposed for energy detection-based non-coherent massive multiple-input multiple-output system. This is motivated by the simple design and high energy efficiency it entails for both the transmitter and receiver.

First, the orthogonal codes is employed to suppress the multi-user interference. However, this comes at the price of consuming more communications resources. In this study, the key to reduce code redundancy is the design of a joint constellation since it makes energy detection applicable when multiple users employ the same orthogonal codes. Although it is unsolvable initially, our analysis indicates that through minimizing the symbol-error rate (SER), the joint constellation design becomes feasible. Concretely, two analytical expressions of SER based on Gamma and Gaussian distributions are derived. Via minimizing the error probability, an important result that the joint constellation should satisfy is obtained. Accordingly, an isometric constellation design is proposed to find constellations that enable non-coherent reception with multiple users, and achieve the minimum SER simultaneously. In addition, decoding regions of symbol decision are optimized to further improve the error performance. In the end, numerical simulations are carried out to highlight the effectiveness of our proposed scheme.

Index Terms

This work was supported by the Fundamental Research Funds for the Central Universities under Grant 2018CDXYTX0011 and the Key Program of Natural Science Foundation of Chongqing under Grant CSTC2017JCYJBX0047. *(Corresponding author: Weiyang Xu)*

H. Q. Xie, W. Y. Xu and B. Li are with the School of Microelectronics and Communication Engineering, Chongqing University, Chongqing, 400044, P. R. China (E-mails: {huiqiangxie, weiyangxu, 20182009113}@cqu.edu.cn).

H. Q. Ngo is with the Institute of Electronics, Communications and Information Technology (ECIT), Queens University Belfast, BT3 9DT, Belfast, U.K., (E-mail: hien.ngo@qub.ac.uk).

Non-coherent massive MIMO, energy detection, constellation design, symbol-error rate (SER).

I. INTRODUCTION

Employing a large number of antennas at base stations (BSs) while sharing the same time-frequency resources, which is known as massive multiple-input multiple-output (MIMO), is a promising technology because of its potential to significantly improve spectral and energy efficiencies [1], [2]. To reap these advantages, it is often assumed that accurate channel state information (CSI) associated with all users is available at BSs. Acquisition of CSI requires the use of orthogonal pilot sequences sending from users. However, the same set of pilots needs to be reused across cells due to insufficient orthogonal pilots in the coverage area. As a result, the channel estimate obtained in a given cell will be corrupted by pilots transmitted by users in the other cells, which makes CSI acquisition much less accurate [3]. In addition, given the massive radio frequency (RF) chains, channel estimation would greatly increase complexity, energy consumption and demands on the front-haul infrastructure [4], [5]. Furthermore, in high mobility environments, the majority of computing resource will be consumed since the coherence interval is quite short. Architectures that use simple, robust and energy efficient designs are thus attractive to realize many of the benefits provided by large antenna systems, especially when it comes to applications of millimeter-wave carrier frequency [6], [7], [8], [9].

Until recently, non-coherent massive single-input multiple-output (SIMO) system, which requires no knowledge of instantaneous CSI at either the transmitter or receiver, has been proposed [10], [11], [12], [13]. Compared with their coherent counterparts, non-coherent receivers enjoy benefits of low complexity, low power consumption and simple structures at the expense of a sub-optimal performance [10]. Among those methods in the literature, energy detection (ED) proves to be promising and has drawn great attention. With a large antenna array, ED could even operate without explicit knowledge of the channel statistics, as signal squaring and averaging performed over the excessive number of receive antennas provides a sample mean-based estimate of the channel energy [11]. In addition, for general channel fading statistics, the performance of ED-based non-coherent communication is the same, in a scaling law sense, as that of the coherent scheme with perfect channel knowledge.

Inspired by the seminal work in [11], the authors in [14] proposed new constellation designs, which are asymptotically optimal with respect to an upper bound of symbol-error rate (SER). Taking both the average and instantaneous channel energy into consideration, two non-coherent

receivers based on ED are proposed in [15]. Besides, bounds on the information rate based on Gaussian approximation are derived, which are tight in low and high signal-to-noise ratio (SNR) regimes [16]. Moreover, the employment of ED-based massive SIMO receiver was proposed in multipath environments [17]. Through utilizing the asymptotic properties brought by massive antennas, signal detection proves to be equivalent to channel equalization, and then a zero-forcing equalizer is employed to remove intersymbol interference. While the above works concentrate on scenarios of SIMO, few researchers consider non-coherent massive MIMO systems. In [11], the authors proposed a joint constellation design for two users, which requires to enumerate all possible ordering that satisfies design constraints. More recently, with ON-OFF keying, the authors have identified the sources of performance degradation, also quantified notions of diversity gain and multiplexing gain in non-coherent massive MIMO systems [18].

According to the literature review, although the ED-based receiver is quite effective in single-user scenario, its application in non-coherent massive MIMO systems is still an open problem. Towards this end, this paper dedicates to the design of an effective non-coherent receiver for the uplink of massive MIMO. The major difference between this study and works in [11] lies in two aspects. First, an upper bound of SER was derived in [11] and both exact and approximate SERs were derived in our study. This makes the constellation design in the next step more accurate and efficient. Second, the two-users constellation design in [11] proves to be NP-Hard to traverse all possible ordering. In contrast, our proposed joint constellation design is able to support multi-user and multi-cell communication. Besides, all users are allowed to simultaneously transmit using the same time-frequency resources in our scheme.

Specifically, the orthogonal codes is reused among cells sufficiently far apart to suppress multi-user interference. However, this could take up extra communication resources. To reduce the code redundancy, users are grouped to share the same orthogonal codes. Hence, the core of this paper is the design of a joint constellation that enables non-coherent communications with multiple users. The main contributions are summarized as follows:

- Our study demonstrates that ED-based non-coherent massive MIMO communications can be achieved by a joint multi-user constellation design.
- To enable ED-based non-coherent multi-user detection and minimize SER at the same time, closed-form expressions of SER based on Gamma and Gaussian distributions are derived. An important condition that the joint constellation needs to satisfy is obtained via minimizing the SER.

- With the aforementioned condition, an isometric constellation design is introduced to find constellations that make ED applicable in scenarios with multiple users. In addition, the optimization of decoding regions is carried out to further reduce the SER.

The rest of this paper is organized as follows. Previous work of non-coherent communications is briefly reviewed in Section II. The framework of ED-based non-coherent massive MIMO system is presented in Section III. Then, problem formulation and SER analysis are discussed in Section IV. Section V details a joint multi-user constellation design. Numerical results are presented to show the performance of ED-based non-coherent massive MIMO communication in Section VI. Finally, Section VII concludes this paper.

$Notation$: $\mathbb{C}^{n\times m}$ and $\mathbb{R}^{n\times m}$ represent complex and real matrices of size $n \times m$, respectively. Bold-font variables denote matrices or vectors. $x \sim \mathcal{CN}(\mu, \sigma^2)$ means random variable x follows a complex Gaussian distribution with mean μ and covariance σ^2. $\mathbb{E}[\cdot]$, Var$[\cdot]$ and $\|\cdot\|_2^2$ denote the expectation, variance and $\mathcal{L}_2$ norm operations, respectively. $(\cdot)^T$ and $(\cdot)^H$ denote the transpose and Hermitian transpose, respectively. $\Re\{\cdot\}$ and $\Im\{\cdot\}$ are the real and imaginary parts of a complex number. erf$(\cdot)$ and erfc$(\cdot)$ are taken to indicate the Gaussian error and complementary Gaussian error functions, respectively. Finally, $\mathbf{a} \otimes \mathbf{b}$ indicates the inner product of vectors $\mathbf{a}$ and $\mathbf{b}$.

II. Previous Work of ED-based Non-coherent Communications in Massive SIMO Systems

To understand the conventional scheme and explain why it does not work in massive MIMO systems, the ED-based non-coherent receiver is briefly reviewed in this section [13], [14].

A. ED-based Non-coherent Massive SIMO Communications

In a massive SIMO system with one transmit antenna and M receive antennas ($M \gg 1$), the $M \times 1$ received signal vector is represented by

$$\mathbf{y} = \mathbf{h}x + \mathbf{v} \tag{1}$$

where x denotes the transmit symbol from a non-negative constellation $\mathcal{P} = \left\{\sqrt{p_1}, \sqrt{p_2}, \ldots, \sqrt{p_N}\right\}$ of size N, $\mathbf{h} = [h_1\ h_2\ \cdots\ h_M]^T \in \mathbb{C}^{M\times 1}$ represents the channel vector with $h_m \sim \mathcal{CN}(0, 1)$ and $\mathbf{v} = [v_1\ v_2\ \cdots\ v_M]^T \in \mathbb{C}^{M\times 1}$ is the noise vector with $v_m \sim \mathcal{CN}(0, \sigma_v^2)$. In this study, channel

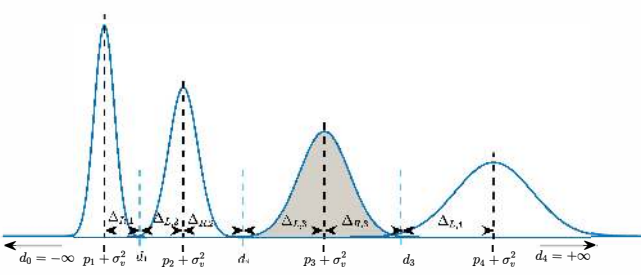

Fig. 1. Decoding regions of a non-negative PAM of size $N = 4$.

and noise vectors are supposed to be mutually independent. The transmit SNR is defined as $\mathbb{E}[x^2]/\mathbb{E}[|v_m|^2]$.

According to the ED principle, after the received signal having been filtered, squared and integrated, the average power across all antennas can be written as

$$\begin{aligned} z &= \frac{1}{M}\mathbf{y}^H\mathbf{y} \\ &= \frac{1}{M}\mathbf{h}^H\mathbf{h}x^2 + \frac{2}{M}\Re\left\{\mathbf{h}^H\mathbf{v}\right\}x + \frac{1}{M}\mathbf{v}^H\mathbf{v}. \end{aligned} \tag{2}$$

When the number of antennas at BS is large enough, the following results are attainable

$$\begin{aligned} \lim_{M\to\infty}\frac{1}{M}\mathbf{h}^H\mathbf{h} &= 1, \\ \lim_{M\to\infty}\frac{1}{M}\mathbf{h}^H\mathbf{v} &= 0, \\ \lim_{M\to\infty}\frac{1}{M}\mathbf{v}^H\mathbf{v} &= \sigma_v^2. \end{aligned} \tag{3}$$

Hence, (2) becomes to

$$\lim_{M\to\infty} z = x^2 + \sigma_v^2. \tag{4}$$

Since M can never be infinite, z approximates to one of the N Gaussian variables depending on *a prior* information of transmit symbols [19]. For example, with non-negative pulse-amplitude modulation (PAM) of $N = 4$, the probability density function (PDF) of z over an additive white Gaussian noise (AWGN) channel is shown in Fig. 1, where $M = 100$ and SNR $= 4$ dB. Four distinct Gaussian-like curves can be observed, corresponding to four constellation points. Provided with the knowledge of channel and noise statistics, the positive line is partitioned into multiple decoding regions $\{d_n\}_{n=0}^{N}$ to decide which symbol was transmitted based on the observation of z, i.e.

$$\widehat{x} = \sqrt{p_n}, \quad \text{if} \quad d_{n-1} \le z < d_n. \tag{5}$$

Concretely, d_0 is $-\infty$ for $\sqrt{p_1}$ and d_N is $+\infty$ for $\sqrt{p_N}$. In the considered system, the non-negative PAM is exploited and $\{d_n\}_{n=1}^{N-1}$ is computed by [11]

$$d_n = \frac{p_n + p_{n+1}}{2} + \sigma_v^2, \quad 1 \leq n \leq N-1. \tag{6}$$

B. ED-based Non-coherent Receiver in Massive MIMO

A simple massive MIMO system, which includes a single cell with two users, is exploited to demonstrate the difficulty the aforementioned non-coherent receiver may encounter. In this case, the composite $M \times 1$ received signal at BS is

$$\mathbf{y} = \mathbf{h}_1 x_1 + \mathbf{h}_2 x_2 + \mathbf{v} \tag{7}$$

where $\mathbf{h}_1, \mathbf{h}_2 \in \mathbb{C}^{M\times 1}$ indicate channel vectors, x_1 and x_2 are transmit symbols from two users. $\mathbf{h}_1$ and $\mathbf{h}_2$ are assumed to be mutually independent, with their items being Gaussian random variables of zero mean and unit variance. As a result, the average power across receive antennas approximates to

$$z = \frac{1}{M}\mathbf{y}^H\mathbf{y} \approx x_1^2 + x_2^2 + \sigma_v^2 \tag{8}$$

when M is sufficiently large. If two users employ the same constellation $\mathcal{P} = \{0, 1\}$, transmit symbols cannot be correctly decoded according to z, for example

$$\begin{aligned} &\text{Case 1 : user 1} \to 1,\ \text{user 2} \to 0 \Rightarrow z \approx 1 + \sigma_v^2, \\ &\text{Case 2 : user 1} \to 0,\ \text{user 2} \to 1 \Rightarrow z \approx 1 + \sigma_v^2. \end{aligned} \tag{9}$$

This specific example shows that although two users transmit different symbols, the ED-based non-coherent receiver cannot be applied because z is not differentiable. Even when different constellations are employed by users, one cannot assure z is always decodable. For instance, in the case of $\mathcal{P}_1 = \left\{0, \sqrt{2}\right\}$ and $\mathcal{P}_2 = \left\{0, 1, \sqrt{2}\right\}$, the indistinguishability in z still exists, namely

$$\begin{aligned} &\text{Case 1 : user 1} \to \sqrt{2},\ \text{user 2} \to 0 \Rightarrow z \approx 2 + \sigma_v^2, \\ &\text{Case 2 : user 1} \to 0,\ \text{user 2} \to \sqrt{2} \Rightarrow z \approx 2 + \sigma_v^2. \end{aligned} \tag{10}$$

The non-orthogonal multiple access (NOMA) can be utilized in symbol detection with multiple users. However, performance of NOMA degrades quickly if the number of users increases. Moreover, NOMA would fail in the situation of (9) or (10) since NOMA relies on the difference in power domain [20]. Therefore, the ED-based non-coherent receiver cannot be directly applied with multiple users, let alone scenarios of multi-cell communications.

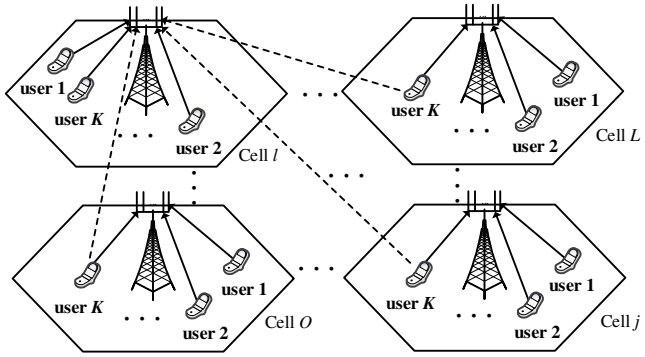

Fig. 2. System model of a multi-cell multi-user massive MIMO system.

III. Non-coherent Massive MIMO Systems

A. System Model

A typical multi-cell massive MIMO system is shown in Fig. 2, where there are L cells, each consisting of one BS with M antennas and K single-antenna users. Users are allowed to simultaneously transmit while sharing the same frequency bands. The $M \times 1$ received signal at the l-th BS is given by

$$\mathbf{y}_l = \mathbf{H}_{ll}\mathbf{x}_l + \sum_{i \neq l} \mathbf{H}_{il}\mathbf{x}_i + \mathbf{v}_l \tag{11}$$

where $\mathbf{H}_{il} = [\mathbf{h}_{il,1}\ \mathbf{h}_{il,2}\ \cdots\ \mathbf{h}_{il,K}] \in \mathbb{C}^{M\times K}$ is the channel matrix between the l-th BS and users in the i-th cell, with items in $\mathbf{h}_{il,k}$ being complex Gaussian random variables of zero mean and variance $\sigma^2_{il,k}$, $\mathbf{x}_i = [x_{i,1}\ x_{i,2}\ \cdots\ x_{i,K}]^T \in \mathbb{R}^{K\times 1}$ denotes transmit symbols of K users in the i-th cell, and $\mathbf{v}_l \in \mathbb{C}^{M\times 1}$ indicates the AWGN, items of $\mathbf{v}_l$ have a variance of σ_v^2.

B. Employment of Orthogonal Codes

The cause of the failure of ED-based non-coherent scheme is the multi-user interference. In coherent systems, this interference can be largely eliminated by detection or precoding algorithms [21]. Here we resort to the orthogonal code, which is widely recognized for its ability to suppress interference [22]. Specifically, if symbols from a certain user are used to modulate a sequence of orthogonal codes unique to that user, symbol detection is then achieved by multiplying received signal with the same codes.

However, orthogonal coding and decoding consume extra resources. To alleviate this issue, we borrow the idea of frequency reuse in cellular network. Hence, adjacent cells must use different

codes, however two cells sufficiently far apart can be assigned with the same codes. Let the codes reuse factor be Q ($Q < L$), then the total available orthogonal codes can be denoted by $\mathbf{W} \in \mathbb{R}^{QK \times QK}$, which is equally partitioned into Q subsets $\mathbf{W}_1, \mathbf{W}_2, \ldots, \mathbf{W}_q, \ldots, \mathbf{W}_Q$, each of size $\mathbb{R}^{K \times QK}$. These subsets obey the following rules

$$\begin{aligned} \mathbf{W}_q \cap \mathbf{W}_{j,j \neq q} &= \varnothing, \\ \mathbf{W}_1 \cup \mathbf{W}_2 \cup \cdots \cup \mathbf{W}_Q &= \mathbf{W}. \end{aligned} \tag{12}$$

The orthogonality requirement of code vectors can be summarized by mathematical representations

$$\begin{aligned} \mathbf{w}_{q,k} \otimes \mathbf{w}_{q,k} &= 1, \\ \mathbf{w}_{q,k} \otimes \mathbf{w}_{q,j(j \neq k)} &= 0, \\ \mathbf{w}_{q,k} \otimes \mathbf{w}_{q',j(q' \neq q)} &= 0 \end{aligned} \tag{13}$$

where $\mathbf{w}_{q,k} \in \mathbb{R}^{1 \times QK}$ is the k-th row of $\mathbf{W}_q$.

Suppose subset $\mathbf{W}_q \in \mathbb{R}^{K \times QK}$ is allocated to the l-th cell, then symbols sent by the k-th user in this cell is first encoded by $\mathbf{w}_{q,k}$, i.e.

$$\mathbf{s}_{l,k} = x_{l,k} \mathbf{w}_{q,k}. \tag{14}$$

Accordingly, the $M \times QK$ received signal at the l-th BS is

$$\mathbf{Y}_l = \mathbf{H}_{ll} \mathbf{S}_l + \sum_{i \neq l} \mathbf{H}_{il} \mathbf{S}_i + \mathbf{V}_l \tag{15}$$

where $\mathbf{V}_l \in \mathbb{C}^{M \times QK}$ indicates the AWGN, and $\mathbf{S}_l \in \mathbb{R}^{K \times QK}$ is created by stacking all $\mathbf{s}_{l,k}$.

As mentioned before, the data of the k-th user in the l-th cell is obtained by right multiplying $\mathbf{Y}_l$ with $\mathbf{w}_{q,k}^T$

$$\mathbf{y}_{l,k} = \mathbf{Y}_l \mathbf{w}_{q,k}^T = x_{l,k} \mathbf{h}_{ll,k} + \widetilde{\mathbf{v}}_{l,k} \tag{16}$$

where $\mathbf{y}_{l,k} \in \mathbb{C}^{M \times 1}$, items of $\widetilde{\mathbf{v}}_{l,k}$ follow complex Gaussian distribution $\mathcal{CN}(0, \sigma_v^2 + \delta)$ where δ denotes the interference from other cells using the same subset $\mathbf{W}_l$. In our study, δ is neglected due to the path-loss. According to ED principle, the decision metric is formulated as the normalized $\mathcal{L}_2$ norm of (16). In the end, the estimate of $x_{l,k}$ is obtained given decoding regions, i.e.

$$\widehat{x}_{l,k} = \sqrt{p_n}, \quad \text{if} \;\; d_{n-1} \leq z_{l,k} < d_n \tag{17}$$

where $z_{l,k}$ denotes the decision metric for the k-th user in the l-th cell, and d_n is computed by

$$d_n = \frac{\sigma_{ll,k}^2 \left(p_n + p_{n+1}\right)}{2} + \sigma_v^2. \tag{18}$$

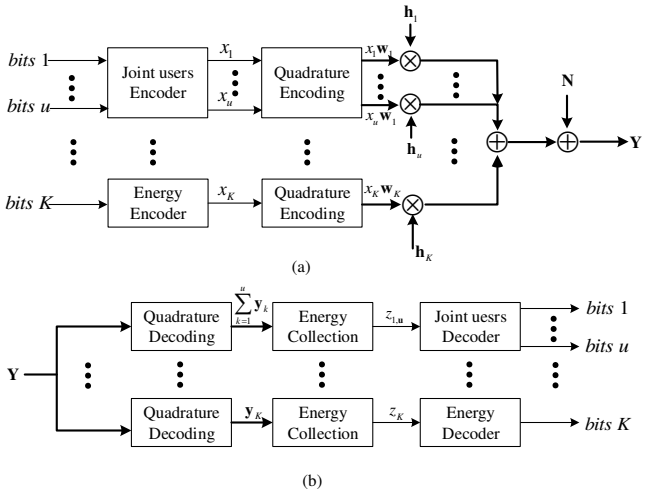

Fig. 3. The structure of a non-coherent massive MIMO system employing constellation design. (a) Transmitter; (b) Receiver.

IV. SER Analysis for Joint Multi-user Constellation Design

The use of orthogonal codes comes at a cost. That is, the code length increases with K, which is unacceptable in real situations. Thus, this paper proposes a joint multi-user constellation design to reduce the code length. Although the formulated problem is unsolvable initially, our study indicates combined with the requirement of constellations that result in the minimum SER, the joint constellation design becomes feasible. Hence, this section concentrates on the derivation of analytical expressions of SER. Before that, the problem to be solved is first presented.

A. Problem Formulation

Intuitively, if the same orthogonal code is used by every U users, the code length reduces from QK to QK/U[1]. However, this can cause the same problem encountered in (9) and (10). The purpose of constellation design is to make the received signal decodable. The structure of non-coherent massive MIMO systems with joint constellation design is shown in Fig. 3.

First of all, K users are equally divided into K/U groups, each with U users. Taking the first group in the l-th cell as an example, let $\mathcal{P}_u = \left\{\sqrt{p_{u,1}}, \sqrt{p_{u,2}}, \ldots, \sqrt{p_{u,N_u}}\right\}$[2] denote the constellation of the u-th user in this group, where $1 \leq u \leq U$ and $\sqrt{p_{u,n_u}}$ is the n_u-th point in

[1]Without loss of generality, K/U is assumed to be an integer.

[2]With the preprocessing in (19), the joint constellations in all groups are identical, thus the group index in omitted here.

$\mathcal{P}_u$ with $1 \leq n_u \leq N_u$. Suppose transmit symbol of the u-th user in the first group is denoted by $x_{l,1,u} = \sqrt{p_{u,n_u}}$, to design the joint constellation off-line, $x_{l,1,u}$ is preprocessed as follows

$$\widetilde{x}_{l,1,u} = \frac{x_{l,1,u}}{\sigma_{ll,1,u}} = \frac{\sqrt{p_{u,n_u}}}{\sigma_{ll,1,u}} \tag{19}$$

where $\sigma^2_{ll,1,u}$ models the channel statistics of the u-th user in the first group. The operation in (19) not only excludes the effect of channel statistics but also simplifies the constellation design. It is worth noting that the amplification of $x_{l,1,u}$ when $\sigma_{ll,1,u}$ is small could violate the transmit power constraint. However, according to (14), the power of $\widetilde{x}_{l,1,u}$ will be reduced by orthogonal coding, ensuring that the violation of power constraint is rare.

As before, assume the reduced subset $\mathbf{W}'_q \in \mathbb{R}^{K/U \times QK/U}$ is allocated to the l-th cell, and the first group employs vector $\mathbf{w}'_{q,1} \in \mathbb{R}^{1 \times QK/U}$. Thus, the resulting $M \times QK/U$ received signal at BS of the l-th cell is given by

$$\mathbf{Y}'_l = \sum_{k=1}^{K/U} \sum_{u=1}^{U} \widetilde{x}_{l,k,u} \mathbf{h}_{ll,k,u} \mathbf{w}'_{q,k} + \sum_{i \neq l} \mathbf{H}_{il} \mathbf{S}'_i + \mathbf{V}'_l \tag{20}$$

where $\mathbf{V}'_l \in \mathbb{C}^{M \times QK/U}$ denotes AWGN with its items being $\mathcal{CN}(0, \sigma_v^2)$, $\mathbf{S}'_i \in \mathbb{R}^{K \times QK/U}$, $\mathbf{h}_{il,k,u}$ is the channel vector from the u-th user of the k-th group in the i-th cell to the l-th BS. Note that the first component on the right hand side of (20) is the signal from the l-th cell, while the second denotes those from other cells. With orthogonal decoding, the data of users in the first group in the l-th cell is obtained by right multiplying $\mathbf{Y}'_l$ with vector $\mathbf{w}'^T_{q,1}$, i.e.

$$\mathbf{y}_{l,\mathbf{U}} = \mathbf{Y}'_l \mathbf{w}'^T_{q,1} \approx \sum_{u=1}^{U} \widetilde{x}_{l,1,u} \mathbf{h}_{ll,1,u} + \mathbf{v}_{l,\mathbf{U}} \tag{21}$$

where $\mathbf{y}_{l,\mathbf{U}} \in \mathbb{C}^{M \times 1}$ and $\mathbf{v}_{l,\mathbf{U}} = \mathbf{V}'_l \mathbf{w}'^T_{l,1}$. The interference from other cells using $\mathbf{W}'_l$ is ignored in (21) due to the path-loss. Clearly, the received signal is composed of data from U users. As before, the decision metric is

$$\lim_{M \to \infty} z = \lim_{M \to \infty} \frac{\|\mathbf{y}_{l,\mathbf{U}}\|_2^2}{M} \approx \sum_{u=1}^{U} p_{u,n_u} + \sigma_v^2. \tag{22}$$

More specifically, there are $\prod_{u=1}^{U} N_u$ possible combinations of $\sum_{u=1}^{U} p_{u,n_u}$ in total, which can be expressed by set $\mathcal{S} = \left\{ s_1, s_2, \ldots, s_{\prod_{u=1}^{U} N_u} \right\}$ with $s_1 = \sum_{u=1}^{U} p_{u,1}$ and $s_{\prod_{u=1}^{U} N_u} = \sum_{u=1}^{U} p_{u,N_u}$. To make it decodable, the condition $s_1 \neq s_2 \neq \cdots \neq s_{\prod_{u=1}^{U} N_u}$ should to be satisfied. Without loss of generality, it is assumed that

$$s_1 < s_2 < \cdots < s_{\prod_{u=1}^{U} N_u}. \tag{23}$$

Therefore, the design of joint multi-user constellation can be modeled as

$$\begin{aligned} \text{Find} \quad & s_1 < s_2 < \cdots < s_{\prod_{u=1}^{U} N_u} \\ \text{s.t.} \quad & \frac{1}{N_u} \sum_{n_u=1}^{N_u} p_{u,n_u} \leq 1,\ 0 \leq p_{u,n_u} < p_{u,n_u+1}, \\ & u = 1, 2, \ldots, U. \end{aligned} \tag{24}$$

However, potential solutions to (24) is countless. It is required to traverse all solutions so that one can find the optimum constellation to minimize the SER, which is NP-hard. Fortunately, our analysis shows that the average SER only relates to constellation points and noise variance. By minimizing the error probability, an extra condition that $\mathcal{S}$ should satisfy can be obtained. Therefore, problem in (24) becomes solvable.

B. Average SER Analysis

The channel and noise statistics are assumed to be known as *a prior*, which is achieved by sending training symbols ahead of data transmission. Since the number of receive antennas is always finite, z in (22) is a random variable. With decision regions $\{d_r\}_{r=0}^{\prod_{u=1}^{U} N_u}$, the probability of correct decision when the composite s_r is sent is denoted by

$$P\left(s_r\right) = \int_{d_{r-1}}^{d_r} f\left(z \left| \sigma_v^2, s_r \right.\right) dz \tag{25}$$

where $f(z\,|\sigma_v^2, s_r\,)$ represents the PDF of z conditioned on σ_v^2 and s_r. The derivation of $f(z\,|\sigma_v^2, s_r\,)$, which is a non-trivial task, is required to calculate the SER. In the following, we employ Gamma and Gaussian random variables to describe the distribution of z.

1) SER Analysis Based on Gamma Distribution:

Proposition 1: Conditioned on σ_v^2 and s_r, the exact distribution of z is given by

$$z \sim \Gamma\left(M, \theta\left(s_r\right)\right) \tag{26}$$

where $\Gamma(M, \theta(s_r))$ is gamma-distributed with shape M and scale factor $\theta(s_r) = \frac{1}{M}(s_r + \sigma_v^2)$.

Proof: The proof can be found in Appendix A. ■

Applying Proposition 1, the cumulative distribution function (CDF) of z is given by

$$F\left(x; M, \theta\left(s_r\right)\right) = \frac{1}{\Gamma\left(M\right)} \gamma\left(M, \frac{x}{\theta\left(s_r\right)}\right)$$

where

$$\gamma\left(M, \frac{x}{\theta\left(s_r\right)}\right) = \int_0^{\frac{x}{\theta(s_r)}} t^{M-1} e^{-t} \mathrm{d}t$$

denotes the lower incomplete Gamma function. Based on (25), the probability of correct decision when s_r is transmitted is represented by

$$P^{\langle\Gamma\rangle}\left(s_r\right) = F\left(d_r; M, \theta\left(s_r\right)\right) - F\left(d_{r-1}; M, \theta\left(s_r\right)\right) \tag{27}$$

where the superscript $\langle\Gamma\rangle$ indicates that the result is obtained with Gamma distribution. Accordingly, the error probability of U users is computed through averaging over all s_r

$$P_e^{\langle\Gamma\rangle} = 1 + \frac{1}{\prod_{u=1}^{U} N_u} \sum_{r=1}^{\prod_{u=1}^{U} N_u} F\left(d_{r-1}; M, \theta\left(s_r\right)\right) - \frac{1}{\prod_{u=1}^{U} N_u} \sum_{r=1}^{\prod_{u=1}^{U} N_u} F\left(d_r; M, \theta\left(s_r\right)\right). \tag{28}$$

Although the analytical SER in (28) is accurate, it is quite complicated due to the presence of lower incomplete Gamma function.

2) SER Analysis Based on Gaussian Distribution Approximation:

Proposition 2: If the number of receive antennas M grows large, then the following approximations are attainable thanks to the Central Limit Theorem (CLT) [23]

$$z = \frac{\left\|\mathbf{y}_{l,\mathbf{U}}\right\|_2^2}{M} \sim \mathcal{N}\left(\mu\left(s_r\right), \sigma^2\left(s_r\right)\right) \tag{29}$$

where

$$\mu\left(s_r\right) = s_r + \sigma_v^2$$
$$\sigma^2\left(s_r\right) = \frac{1}{M}\left(s_r + \sigma_v^2\right)^2.$$

Proof: The proof can be found in Appendix B. ■

According to Lemma 2 and the CDF of Gaussian distribution, (25) can be rewritten as

$$P^{\langle G\rangle}\left(s_r\right) = \frac{1}{2}\left(\text{erf}\left(\frac{\Delta_{L,r}}{\sqrt{2}\sigma\left(s_r\right)}\right) + \text{erf}\left(\frac{\Delta_{R,r}}{\sqrt{2}\sigma\left(s_r\right)}\right)\right) \tag{30}$$

where $\Delta_{L,r} = \mu(s_r) - d_{r-1}$ and $\Delta_{R,r} = d_r - \mu(s_r)$, the superscript $\langle G\rangle$ indicates that the result is obtained by Gaussian distribution approximation.

In the same way, the probability of errors based on Gaussian distribution approximation can be calculated by averaging over all s_r, i.e.

$$\begin{aligned} P_e^{\langle G\rangle} &= 1 - \frac{1}{\prod_{u=1}^{U} N_u} \sum_{r=1}^{\prod_{u=1}^{U} N_u} P^{\langle G\rangle}\left(s_r\right) \\ &= \frac{1}{2\prod_{u=1}^{U} N_u} \sum_{r=1}^{\prod_{u=1}^{U} N_u} \text{erfc}\left(\frac{\Delta_{L,r}}{\sqrt{2}\sigma\left(s_r\right)}\right) + \frac{1}{2\prod_{u=1}^{U} N_u} \sum_{r=1}^{\prod_{u=1}^{U} N_u} \text{erfc}\left(\frac{\Delta_{R,r}}{\sqrt{2}\sigma\left(s_r\right)}\right). \end{aligned} \tag{31}$$

It is observed that $P_e^{\langle G\rangle}$ relates to M, s_r and noise variance σ_v^2. Since σ_v^2 is an environmental parameter, one can minimize error rate by optimizing the joint constellation if M is fixed.

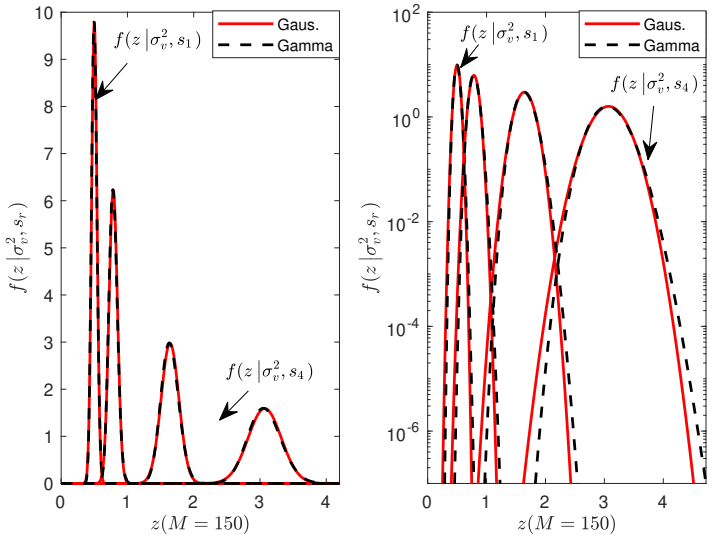

Fig. 4. $f\left(z\,|\sigma_v^2, s_r\right)$ derived from Gamma and Gaussian distributions.

Fig. 4 illustrates the results in (28) and (31), with two sub-figures using linear and logarithmic coordinates, respectively. Although the curve employing Gaussian distribution on linear coordinate matches well with the accurate distribution, obvious discrepancy between these two is observed on logarithmic coordinate. This difference could result in mismatching between the SER in (31) and simulation results, as will be elaborated in Section VI.

V. Joint Multi-user Constellation Design and Decision Region Optimization

In this section, the condition that constellations must satisfy to minimize the error rate is derived. Then combined with this result, a joint multi-user constellation is proposed.

A. Minimization of SER

The analytical result of SER based on Gaussian approximation is selected in the following analysis due to its mathematical tractability. However, both (28) and (31) will be included in numerical simulation.

It can be revealed from (31) that the error probability lowers down with the decrease of $\sigma(s_r)$, which relates to s_r. This observation, coupled with the relationship between SER and $\Delta_{L,r}$ or $\Delta_{R,r}$, clearly demonstrates the potential to reduce the error probability via optimizing the joint constellation $\mathcal{S}$. However, this optimization problem cannot be solved directly. Alternatively, we minimize the upper boundary of SER and turn the original problem into solvable but sub-optimal.

Specifically, the upper bound of SER P_e^U is shown as

$$\begin{aligned} P_e &= 1 - \frac{1}{2\prod_{u=1}^{U} N_u} \sum_{r=1}^{\prod_{u=1}^{U} N_u} \left(\text{erf}\left(\frac{\Delta_{L,r}}{\sqrt{2}\sigma\left(s_r\right)} \right) + \text{erf}\left(\frac{\Delta_{R,r}}{\sqrt{2}\sigma\left(s_r\right)} \right) \right) \\ &\leq 1 - \frac{1}{2\prod_{u=1}^{U} N_u} \sum_{r=1}^{\prod_{u=1}^{U} N_u} \left(\text{erf}\left(\frac{\Delta_{L,r}}{\sqrt{2}\sigma\left(s_{\prod_{u=1}^{U} N_u}\right)} \right) + \text{erf}\left(\frac{\Delta_{R,r}}{\sqrt{2}\sigma\left(s_{\prod_{u=1}^{U} N_u}\right)} \right) \right) = P_e^U. \end{aligned} \tag{32}$$

As a consequence, the problem of minimizing the upper bound of SER can be formulated as

$$\begin{aligned} \min_{\{\mathcal{S}\}} \quad & P_e^U \\ \text{s.t.} \quad & \frac{1}{N_u} \sum_{n_u=1}^{N_u} p_{u,n_u} \leq 1, \ 0 \leq p_{u,n_u} < p_{u,n_u+1}, \\ & u = 1, 2, \ldots, U. \end{aligned} \tag{33}$$

According to (30) and (32), the upper bound of correct decision probability of a single s_r is computed by

$$P^U(s_r) = \frac{1}{2}\text{erf}\left(\frac{\Delta_{L,r}}{\sqrt{2}\sigma\left(s_{\prod_{u=1}^{U} N_u}\right)} \right) + \frac{1}{2}\text{erf}\left(\frac{\Delta_{R,r}}{\sqrt{2}\sigma\left(s_{\prod_{u=1}^{U} N_u}\right)} \right). \tag{34}$$

Obviously, minimizing the average SER equals to maximizing the average probability of correct decision, thus (33) translates to

$$\begin{aligned} \max_{\{\mathcal{S}\}} \quad & \frac{1}{\prod_{u=1}^{U} N_u} \sum_{r=1}^{\prod_{u=1}^{U} N_u} P^U(s_r) \\ \text{s.t.} \quad & \frac{1}{N_u} \sum_{n_u=1}^{N_u} p_{u,n_u} \leq 1, \ 0 \leq p_{u,n_u} < p_{u,n_u+1}, \\ & u = 1, 2, \ldots, U. \end{aligned} \tag{35}$$

In order to find the constellation that results in the minimum SER, the main ideas behind are

1 There are many constellations that can meet the power constraint. Thus, let's assume constellations that satisfy the power constraint form the set $\mathcal{S}$, then the power constraint can be removed from the optimization problem. Therefore, the original problem translates to optimize the decoding regions $\Delta_{L,r}$ and $\Delta_{R,r}$ to minimize the SER.

2 When relationships between $\Delta_{L,r}$ and $\Delta_{R,r}$ are obtained, one can find the constellation in set $\mathcal{S}$ that meets those relationships. Thus the optimal constellation is finally obtained.

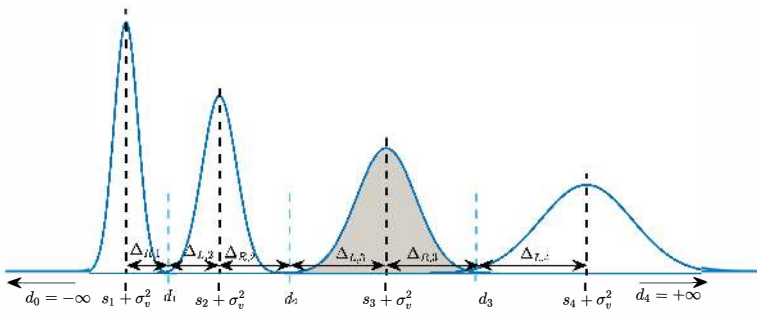

Fig. 5. Decoding regions for our proposed joint constellation with two users.

From [19], the upper bound of average probability of correct decision given in (35) is convex in the space spanned by $\mathcal{S}$. Accordingly, for each s_r, $P^U(s_r)$ is maximized if

$$\text{erf}\left(\frac{\Delta_{L,r}}{\sqrt{2}\sigma\left(s_{\prod_{u=1}^{U} N_u}\right)}\right) = \text{erf}\left(\frac{\Delta_{R,r}}{\sqrt{2}\sigma\left(s_{\prod_{u=1}^{U} N_u}\right)}\right) \tag{36}$$

which is equivalent to the following result

$$\Delta_{L,r} = \Delta_{R,r}. \tag{37}$$

As an example, Fig. 5 draws the decoding regions of the proposed joint constellation with two users. Take $s_2 + \sigma_v^2$ and $s_3 + \sigma_v^2$ in this figure for instance, when subtracting the first from the second, it is obtained that $s_3 - s_2 = \Delta_{L,3} + \Delta_{R,2}$. Moreover, this relationship can be generalized to

$$s_r - s_{r-1} = \Delta_{L,r} + \Delta_{R,r-1}. \tag{38}$$

Hence, optimization problem in (35) can be rewritten as

$$\begin{aligned} \max_{\{\mathcal{S}\}} \quad & \frac{1}{\prod_{u=1}^{U} N_u} \sum_{r=1}^{\prod_{u=1}^{U} N_u} P^U(s_r) \\ \text{s.t.} \quad & s_r - s_{r-1} = \Delta_{L,r} + \Delta_{R,r-1}, \end{aligned} \tag{39}$$

For each r, $\sum_{r=1}^{\prod_{u=1}^{U} N_u} P^U(s_r)$ is separable. Therefore, (39) is divided into $\prod_{u=1}^{U} N_u$ individual optimization problems

$$\begin{aligned} \max_{\{s_r, s_{r-1}\}} \quad & \text{erf}\left(\frac{\Delta_{L,r}}{\sqrt{2}\sigma\left(s_{\prod_{u=1}^{U} N_u}\right)}\right) + \text{erf}\left(\frac{\Delta_{R,r-1}}{\sqrt{2}\sigma\left(s_{\prod_{u=1}^{U} N_u}\right)}\right) \\ \text{s.t.} \quad & s_r - s_{r-1} = \Delta_{L,r} + \Delta_{R,r-1}, \\ & u = 1, 2, \ldots, U. \end{aligned} \tag{40}$$

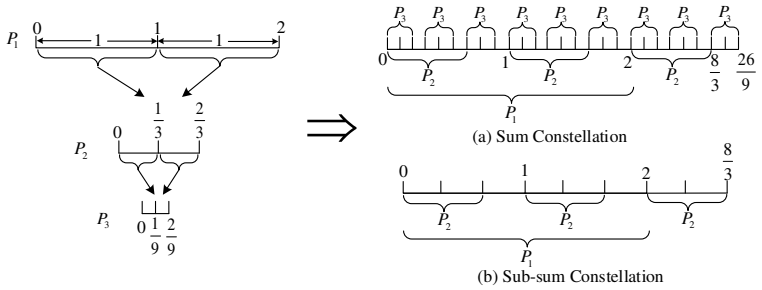

Fig. 6. The flow chart of a simple joint multi-user constellation design, where $\prod_{u=1}^{3} N_u = 27$.

According to the convex property of $\mathrm{erf}(x)$ and Cauchy-Schwarz inequality [24], each convex optimization problem in (40) is solved by

$$\mathrm{erf}\left(\frac{\Delta_{L,r}}{\sqrt{2}\sigma\left(s_{\prod_{u=1}^{U} N_u}\right)}\right) = \mathrm{erf}\left(\frac{\Delta_{R,r-1}}{\sqrt{2}\sigma\left(s_{\prod_{u=1}^{U} N_u}\right)}\right). \tag{41}$$

Thus, the following result is able to be obtained

$$\Delta_{L,r} = \Delta_{R,r-1}. \tag{42}$$

Combining (37) and (42), it is derived that constellations leading to the minimum SER should meet the condition

$$s_2 - s_1 = s_3 - s_2 = \cdots = s_{\prod_{u=1}^{U} N_u} - s_{\prod_{u=1}^{U} N_u - 1}. \tag{43}$$

B. Design of Joint Multi-user Constellation

According to (43), the original joint multi-user constellation design in (24) changes to

$$\begin{aligned} \text{Find} \quad & s_1 < s_2 < \cdots < s_{\prod_{u=1}^{U} N_u} \\ \text{s.t.} \quad & s_2 - s_1 = s_3 - s_2 = \cdots = s_{\prod\limits_{u=1}^{U} N_u} - s_{\prod\limits_{u=1}^{U} N_u - 1}, \\ & \frac{1}{N_u}\sum_{n_u=1}^{N_u} p_{u,n_u} \le 1,\ 0 \le p_{u,n_u} < p_{u,n_u+1}, \\ & u = 1, 2, \ldots, U. \end{aligned} \tag{44}$$

To find the solution to (44), an isometric constellation design is provided in the following proposition.

Proposition 3: A joint multi-user isometric constellation is proposed to solve (44), the result is shown as follows

$$\begin{aligned}
\mathcal{P}_1 &= \left\{0, \sqrt{\frac{2\times 1}{N_1-1}}, \sqrt{\frac{2\times 2}{N_1-1}}, \ldots, \sqrt{\frac{2\left(N_1-1\right)}{N_1-1}}\right\},\\
\mathcal{P}_2 &= \left\{0, \sqrt{\frac{2\times 1}{\left(N_1-1\right)N_2}}, \sqrt{\frac{2\times 2}{\left(N_1-1\right)N_2}}, \ldots, \sqrt{\frac{2\left(N_2-1\right)}{\left(N_1-1\right)N_2}}\right\},\\
&\vdots\\
\mathcal{P}_U &= \left\{0, \sqrt{\frac{2\times 1}{\left(N_1-1\right)\prod_{u=2}^{U} N_u}}, \sqrt{\frac{2\times 2}{\left(N_1-1\right)\prod_{u=2}^{U} N_u}}, \ldots, \sqrt{\frac{2\left(N_u-1\right)}{\left(N_1-1\right)\prod_{u=2}^{U} N_u}}\right\}
\end{aligned} \tag{45}$$

where the size of the first constellation $\mathcal{P}_1$ is the smallest.

Proof: The proof can be found in Appendix C. ■

The design flow chart of the proposed joint 3-user constellation is illustrated in Fig. 6, where $\prod_{u=1}^{3} N_u = 27$ with $N_{1,2,3} = 3$. The characteristics of this design are summarized below.

- The essence of (45) is that points of previous constellation are equally spaced. Then the next constellation is designed within the area between two adjacent points of the previous one, and to ensure that the constellation after next can be designed in the same way.
- All isometric constellations $\{\mathcal{P}_1, \mathcal{P}_2, \ldots, \mathcal{P}_U\}$ constitute the overall constellation $\mathcal{S}$. Each element in $\mathcal{S}$ is unique. Similarly, any two or more isometric constellations are combined as a sub-sum constellation if needed.
- The isometric constellation can be considered as a new finite-alphabet NOMA to allocate transmit power among multiple users [25].
- Since the probability of symbol errors is an increasing function of U[3], one should be careful to select the number of users sharing the same orthogonal code to strike a balance between system performance and complexity. For example, given a fixed number of users, how to achieve a predefined SER with the least amount of orthogonal codes is interesting, which needs further study.

C. A Case Study

An example is listed to illustrate how does the joint constellation design realize symbol detection of multiple users simultaneously. Concretely, suppose the system under consideration

[3]The proof can be found in Appendix D.

includes one multi-antenna BS and two single-antenna users. By applying (45), the constellations of user 1 and 2 are separately given by

$$\mathcal{P}_1 = \left\{0, 1, \sqrt{2}\right\}, \quad \mathcal{P}_2 = \left\{0, \sqrt{\frac{1}{3}}, \sqrt{\frac{2}{3}}\right\}. \tag{46}$$

The received signal is the same as in (7). At the BS, the receiver calculates the average power of the composite received signal $\mathbf{y}$

$$\lim_{M\to\infty} z = \lim_{M\to\infty} \frac{\|\mathbf{y}\|_2^2}{M} \approx x_1^2 + x_2^2 + \sigma_v^2 \tag{47}$$

where $x_{l,1} \in \mathcal{P}_1$ and $x_{l,2} \in \mathcal{P}_2$.

There are nine possible values of $x_1^2 + x_2^2$, namely

$$x_1^2 + x_2^2 \in \left\{0, \frac{1}{3}, \frac{2}{3}, 1, \frac{4}{3}, \frac{5}{3}, 2, \frac{7}{3}, \frac{8}{3}\right\}. \tag{48}$$

Obviously, elements in (48) are different from each other. If the noise is ignored, transmit symbols of user 1 and 2 can be recognized simply according to the observation of z, for example

$$\begin{aligned} &\text{Case } 1: z \approx \frac{5}{3} \Rightarrow \text{user } 1 \to 1, \text{user } 2 \to \sqrt{\frac{2}{3}}, \\ &\text{Case } 2: z \approx \frac{7}{3} \Rightarrow \text{user } 1 \to \sqrt{2}, \text{user } 2 \to \sqrt{\frac{1}{3}}. \end{aligned} \tag{49}$$

Therefore, the proposed joint constellation not only realizes non-coherent multi-user detection, but also reduces the coding cost.

D. Optimization of Decoding Regions

For a fixed isometric constellation, the SER can be further reduced by optimizing the decoding regions. Let $\mathcal{D} = \left\{d_1, d_2, \ldots, d_{\prod_{u=1}^{U} N_u}\right\}$, thus instead of using (6), the optimized decision regions are computed via solving the following optimization problem

$$\begin{aligned} \max_{\{\mathcal{D}\}} \quad & \frac{1}{\prod_{u=1}^{U} N_u} \sum_{r=1}^{\prod_{u=1}^{U} N_u} P\left(s_r, d_r\right) \\ \text{s.t.} \quad & s_r - s_{r-1} = \Delta_{L,r}\left(d_{r-1}\right) + \Delta_{R,r-1}\left(d_{r-1}\right) \end{aligned} \tag{50}$$

where $P(s_r, d_r)$ is the probability of correct decision conditioned on s_r and d_r.

Proposition 4: With different SNR, the decision regions can be defined by

$$d_r = \mu\left(s_r\right) + \frac{\left(s_r + \sigma_v^2\right)\left(s_{r+1} - s_r\right)}{s_{r+1} + s_r + 2\sigma_v^2} \tag{51}$$

where $d_0 = -\infty$ and $d_{\prod_{u=1}^{U} N_u} = +\infty$.

Proof: For each r, $\frac{1}{\prod_{u=1}^{U} N_u} \sum_{r=1}^{\prod_{u=1}^{U} N_u} P(s_r, d_r)$ in (50) are separable. As a result, it is decomposed into $\prod_{u=1}^{U} N_u$ individual optimization problems

$$\begin{aligned} \max_{\{d_{r-1}\}} \quad & \text{erf}\left(\frac{\Delta_{L,r}\left(d_{r-1}\right)}{\sqrt{2}\sigma\left(s_r\right)}\right) + \text{erf}\left(\frac{\Delta_{R,r-1}\left(d_{r-1}\right)}{\sqrt{2}\sigma\left(s_{r-1}\right)}\right) \\ \text{s.t.} \quad & s_r - s_{r-1} = \Delta_{L,r}\left(d_{r-1}\right) + \Delta_{R,r-1}\left(d_{r-1}\right). \end{aligned} \tag{52}$$

Since the error function is convex in the range of $(0, \infty)$, (52) is solved by

$$\text{erf}\left(\frac{\Delta_{L,r}\left(d_{r-1}\right)}{\sqrt{2}\sigma\left(s_r\right)}\right) = \text{erf}\left(\frac{\Delta_{R,r-1}\left(d_{r-1}\right)}{\sqrt{2}\sigma\left(s_{r-1}\right)}\right). \tag{53}$$

Thus, the following result is able to be obtained

$$\frac{\Delta_{R,r-1}\left(d_{r-1}\right)}{\sqrt{2}\sigma\left(s_{r-1}\right)} = \frac{\Delta_{L,r}\left(d_{r-1}\right)}{\sqrt{2}\sigma\left(s_r\right)} = \frac{s_r - s_{r-1}}{\sqrt{2}\sigma\left(s_{r-1}\right) + \sqrt{2}\sigma\left(s_r\right)}. \tag{54}$$

Both $\Delta_{R,r-1}$ and $\Delta_{L,r}$ can be used to calculate the decision regions. If $\Delta_{R,r-1}$ is selected, the optimization is completed by $d_r = \mu\left(s_{r+1}\right) - \Delta_{L,r+1}\left(d_r\right)$. Hence, the result shown in Proposition 4 is obtained. ■

If the required SER is predefined, the same orthogonal codes can be shared by more users since the threshold optimization could reduce the probability of error.

E. Users Grouping

In the analysis above, all users in one cell are divided into groups equally. We will show that the average grouping is optimal with respect to reduce the error rate.

Proposition 5: Suppose there are k_l users in the l-th group, $\sum_{l=1}^{L} k_l = K$. Let $f(k_l)$ indicate the average SER of l-th group. Then the minimum error probability is achieved if and only if

$$k_1 = k_2 = \cdots = k_L \tag{55}$$

Proof: The average SER of the whole cell is denoted by $\frac{1}{L}\sum_{l=1}^{L} f(k_l)$. Hence, the optimal grouping that could minimize the SER can be formulated as

$$\begin{aligned} \min_{\{k_1, k_2, \ldots, k_L\}} \quad & \frac{1}{L}\sum_{l=1}^{L} f(k_l) \\ \text{s.t.} \quad & \sum_{l=1}^{L} k_l = K \end{aligned} \tag{56}$$

It is worth noting that $f(k_l)$ is composed of $\text{erfc}(k_l)$, which is convex if $k_l > 0$. Therefore, the problem in (56) can be solved with the following lemma.

Lemma 1: For a real convex function φ, numbers $x_1, x_2, \ldots, x_n$ in its domain, and positive weights a_i, Jensen's inequality can be stated as

$$\varphi\left(\frac{\sum a_i x_i}{\sum a_i}\right) \leq \frac{\sum a_i \varphi(x_i)}{\sum a_i} \tag{57}$$

where the equality holds if and only if $x_1 = x_2 = \cdots = x_n$ or φ is linear [24].

If we set $a_i = 1$, the Jensen's inequality can be rewritten as

$$\varphi\left(\frac{\sum x_i}{n}\right) \leq \frac{\sum \varphi(x_i)}{n} \tag{58}$$

where the equality holds if and only if $x_1 = x_2 = \cdots = x_n$ or φ is linear. From Lemma 1 and (58), $\frac{1}{L}\sum_{l=1}^{L} f(k_l)$ achieves its minimum when $k_1 = k_2 = \cdots = k_L$. Therefore, proposition 5 is obtained. ■

VI. Design Considerations: Complexity and Performance

We now provide a short discussion on two important design considerations which are essential to understand the feasibility of the suggested system: the complexity involved in computing the constellations and the comparison with the non-negative PAM.

A. Complexity

The isometric design criterion provides the closed-form expression, which means that it could actually be executed off-line with look-up tables in the transceiver. For example, when a new user joins the network, it can get the constellation automatically instead of recomputing the constellations and reassigning to all users. Besides, within performance tolerance, the isometric design saves the time used for computing constellation real-time compared with other algorithms, which reduces the end-to-end latency and is promising in applications of Ultra-reliable low-latency communication (uRLLC).

B. Comparison with conventional PAM

The isometric constellation also fully exploits the degree of freedom compared with conventional non-negative PAM. Fig. 7 gives an example of joint constellations with two users according to non-negative PAM criterion and isometric design criterion, respectively. P_1 and P_2 separately denote the constellations of user 1 and 2. In this scenario, we not only take single user's performance into consideration, but also the overall performance.

It is observed that although P_1 in Fig. 8(a) can obtain a better performance than that in Fig. 8(b). However, the joint non-negative PAM criterion does not fully exploit the distance between neighboring constellation points, i.e., the distance between $\frac{13}{15}$ and $\frac{12}{5}$. In contrary, the isometric criterion utilizes the distance in a more efficient way. This difference can be also observed from Fig. 8, where we draw the distributions of received signal in the case of constellation of eight points. Clearly, the overlap regions between neighboring distributions are more remarkable in Fig. 8(a) than Fig. 8(b). Even if these overlaps can be reduced by increasing the number of antennas, it comes at a huge cost. On the other hand, the isometric design criterion improves the over all performance greatly.

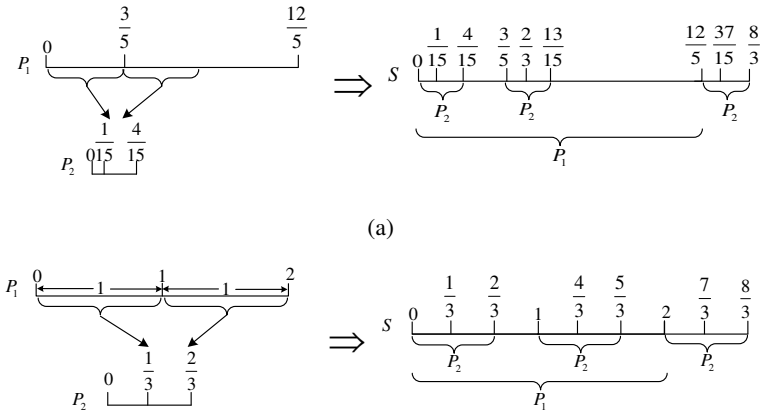

Fig. 7. The flow chart of a simple joint multi-user constellation design: (a) Joint PAM constellation, (b) Joint isometric constellation.

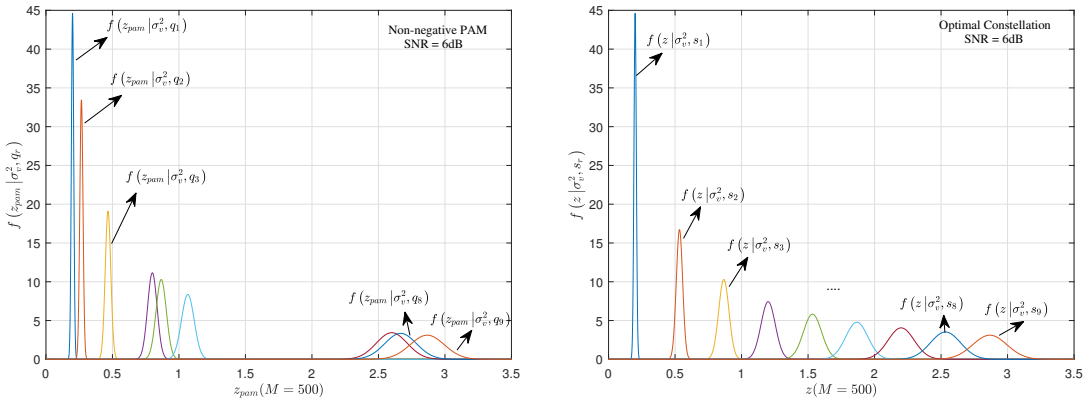

Fig. 8. The PDF of joint constellation: (a) joint PAM constellation, (b) joint isometric constellation.

VII. Numerical Results

This section will present results obtained via Monte Carlo simulations and theoretical results to show the effectiveness of the proposed non-coherent scheme. In all examples, C indicates the code length. The large-scale fading is computed using the free-space propagation model. Besides, PAM refers to the non-negative PAM, that is

$$\mathcal{P} = \{\sqrt{p_1}, \sqrt{p_2}, \ldots, \sqrt{p_N}\} \tag{59}$$

where its n-th entry is $\sqrt{p_n} = n\sqrt{\varepsilon}$ with ε being a normalization constant.

A. Estimation of Channel and Noise Statistics

Our proposed scheme relies on a prior knowledge of σ_v^2 and $\sigma_{ll,k}^2$, which need to be estimated before data transmission. In the case of no joint constellation, if users do not send any data, the received matrix of size $M \times QK$ only contains the noise. Considering the received signal in (15), the noise variance can be calculated by

$$\widehat{\sigma}_v^2 = \frac{\left\|\mathbf{V}_l \mathbf{w}_{l,1}^T\right\|_2^2}{M}. \tag{60}$$

On the other hand, if all users transmit symbol "1", the channel statistics of the k-th user in the l-th cell is shown as

$$\widehat{\sigma}_{ll,k}^2 = \frac{\left\|\mathbf{Y}_l \mathbf{w}_{l,k}^T\right\|_2^2}{M} - \widehat{\sigma}_v^2. \tag{61}$$

Note that (60) and (61) are also applicable in the multi-cell scenario.

If the joint constellation among multiple users is exploited, one can still follow the way of (60). As for the channel statistics, u users are required to send an identity matrix $\mathbf{I}_{u\times u}$, of which columns are assigned to each user one-by-one. It can be shown that only one user sends data in each time interval, while data of the others gets nulled. Thus, (61) can be applied to estimate the channel statistics.

Fig. 9 illustrates the mean square error (MSE) of (61) versus M in a single-cell multi-user massive MIMO system with $C = 8$. The estimate of channel statistics in the case of no noise is included as the benchmark. From the simulation results, when M grows, the MSE significantly decreases due to the channel uncertainty gradually disappears. In addition, this method shows good performance even at low SNR. For example, the MSE obtained at SNR $= 0$ dB is almost identical to the benchmark.

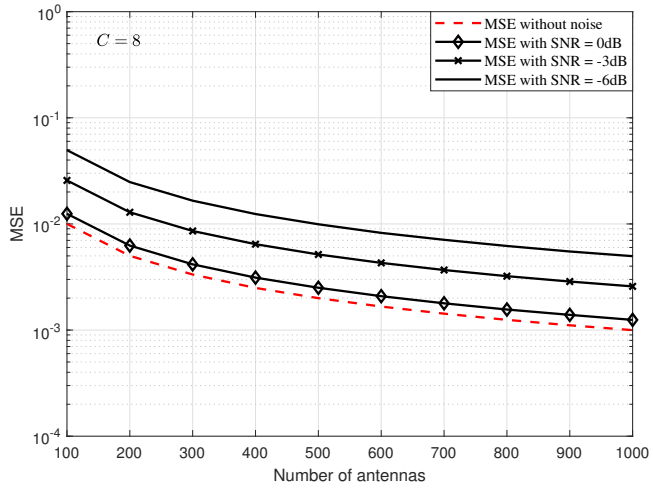

Fig. 9. MSE of (61) versus M for a single cell multi-user massive MIMO system with various SNRs, where $K = 8$ and $C = 8$.

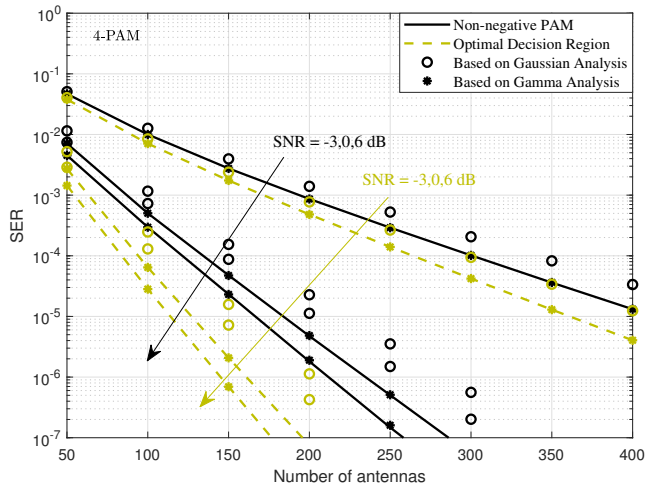

Fig. 10. SER versus M in a single cell massive MIMO system, where $C = 8$.

B. Single-Cell Scenarios

Fig. 10 and Fig. 11 separately draw the relation between the SER with respect to M and SNR in a single-cell system. Both analytical results of (31) and (28) are included for comparison. Fig. 10 demonstrates the logarithm of SER decreases almost linearly along with M, which again proves the advantage of massive antenna array. Moreover, it is found that the rate of descent of SER versus M becomes larger at higher SNRs. In addition, the expression in (28) fits the numerical results rather well in the whole range of M. However, a noticeable difference between (31) and numerical results appears when M is large, which arises from the mismatch between

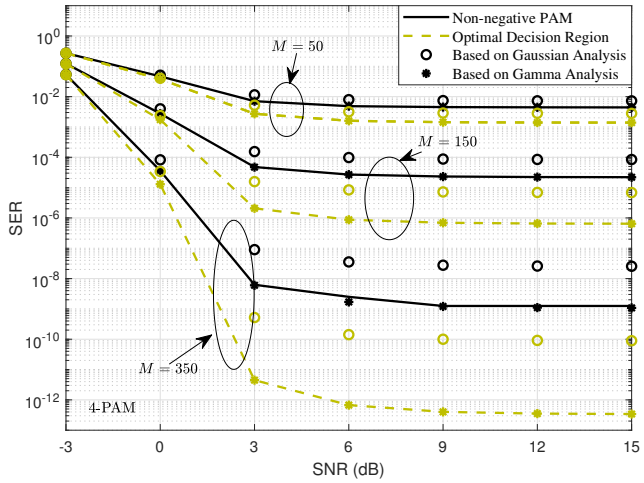

Fig. 11. SER versus SNR in a single cell massive MIMO system, where $C = 8$.

the actual distribution and Gaussian approximation. On the other hand, Fig. 11 indicates the non-coherent system performs well at low SNRs. As before, the analytical results using Gamma distribution are quite accurate and can be employed as a fine prediction model of SER. Although increasing M could reduce the error floor, it comes at the price of implementation cost. Therefore, more attention should be paid to address the balance between system performance and cost.

Furthermore, both Fig. 10 and Fig. 11 indicate the optimized decision regions in Proposition 4 can reduce the number of errors remarkably. Since d_r is able to be calculated before data transmission, Proposition 4 proves to be another efficient way to reduce code length aside from constellation design.

C. Multi-cell Scenarios

The considered system model includes 19 cells with each accommodating $K = 20$ users. The joint constellation design with optimal decision regions is employed.

Fig. 12 demonstrates the relationship between SER and M at SNR $= -3$ dB and -6 dB. Three modulation schemes are employed, namely a non-negative 4-PAM, a joint constellation of 2 users with $N_{1,2} = 2$ and that of 4 users with $N_{1,2,3,4} = 2$. Likewise, the proposed SER expression based on Gamma distribution fits well with the numerical results in the multi-cell scenario. As the number of joint users increases, the code length is reduced and the system performance gradually deteriorate. It is caused by the fact that transmit power is not fully utilized in joint constellation design. This observation conforms to our analysis that in essence, the joint

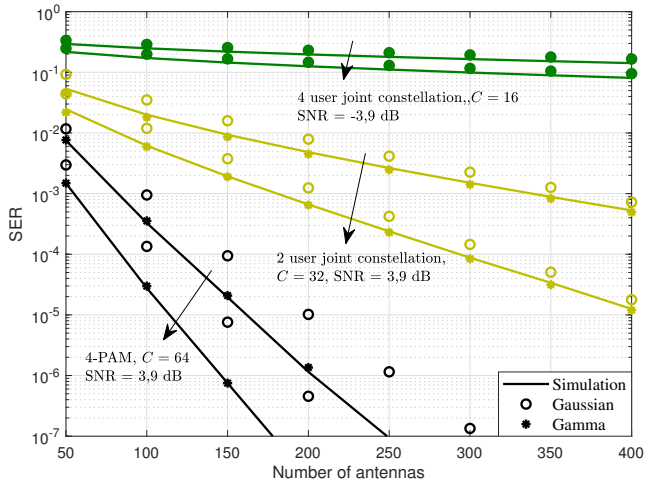

Fig. 12. SER versus M in multi-cell massive MIMO systems, where $L = 19$, and the joint multi-user constellation with optimal decision regions is employed.

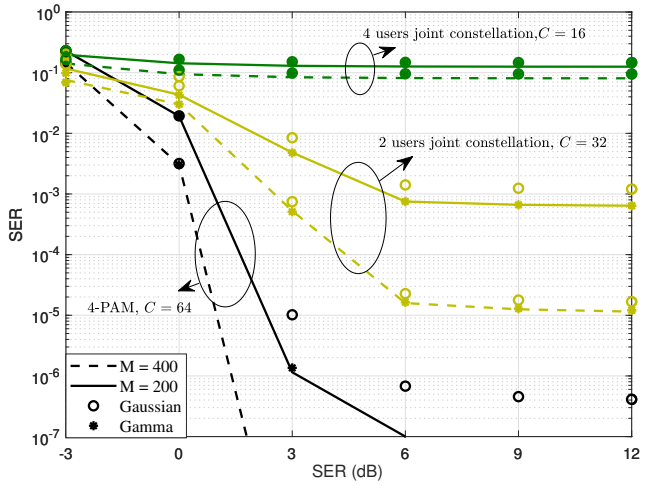

Fig. 13. SER versus SNR in multi-cell massive MIMO systems, where $L = 19$, and the joint multi-user constellation with optimal decision regions is employed.

constellation design sacrifices performance for lower implementation cost. Similarly, the SER approximately scales down with the increase of M and the slope of SER with respect to M becomes larger at higher SNRs. However, the improvement of error performance by increasing M when the joint constellation of 4 users is employed is almost negligible.

Fig. 13 reports the simulated SER versus the SNR. Specifically, the system performs well at low SNR. For example, when $M = 400$ and $C = 64$, it only requires SNR $= 1$ dB to achieve SER $= 10^{-5}$. As before, an error floor appears at high SNR regions, and it becomes lower when

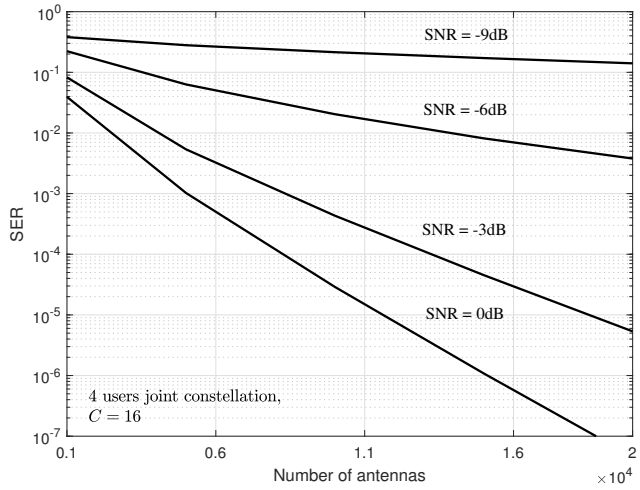

Fig. 14. Theoretical SER based on Gamma distribution versus M in multi-cell massive MIMO systems, where $L = 19$, a joint constellation with 4 users is employed.

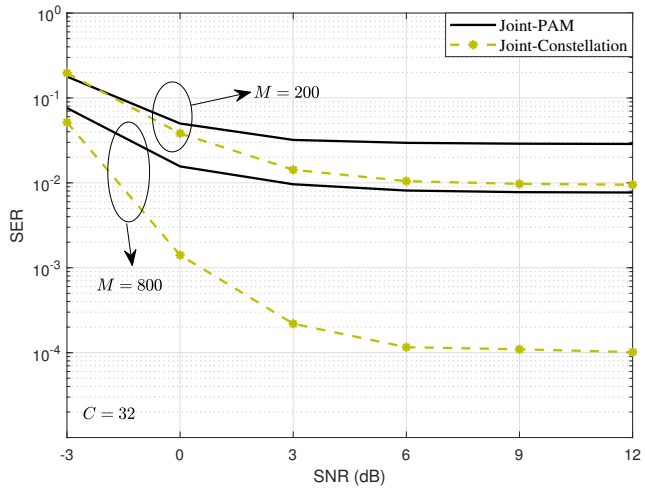

Fig. 15. SER comparison between the proposed joint constellation and joint-PAM with 2 users, where $N_1 = 2$ and $N_2 = 3$.

the number of antennas grows. Moreover, Fig. 14 draws the theoretical SER based on Gamma distribution versus M in multi-cell massive MIMO systems, where a joint constellation with 4 users is employed. Though the performance of joint 4-user constellation is not well in Fig. 12 and Fig. 13, Fig. 14 indicates the SER can be constantly reduced by increasing M. Therefore, those results is able to be utilized to predict the performance if numerical simulation is difficult to conduct.

Fig. 15 compares the proposed joint constellation and joint-PAM with 2 users, where $N_1 = 2$

and $N_2 = 3$. Joint PAM represents a joint multi-user non-negative PAM constellation, obtained by using non-negative criteria in (59) and joint multi-user criteria in Fig. 6. It is worth noting that points of previous constellation are equally spaced in our design, while in joint-PAM, points are set using PAM constellations. With the same code length, our proposed constellation leads to a better performance compared with the joint-PAM. For example, the SER of our design with $M = 200$ approximately equals to that of joint-PAM when $M = 800$. From another point of view, to meet the required SER, the proposed constellation can save a large amount of resources by reducing the number of antennas.

VIII. Conclusion

This paper proposed a new joint multi-user constellation in ED-based non-coherent massive MIMO system. In order to suppress the multi-user interference, the orthogonal codes was employed. However, the encoding and decoding takes up extra resources.

To reduce code redundancy, multiple users were grouped together and assigned with the same orthogonal codes. Therefore, what we focus on was to find constellations that make the received signal decodable in this scenario. Through deriving and minimizing the error probability, an important result that the joint constellation should meet was obtained. Afterwards, a joint multi-user constellation was designed and decode regions of symbol decision were optimized. Analytical results showed the number of users sharing the same codes is critical to the error performance, which is required to be paid attention in system design. Numerical results proved the effectiveness of the proposed joint multi-user constellation design.

Appendix A
Proof of proposition 1

The distribution of $\left|[\mathbf{y}_{l,\mathbf{U}}]_m\right|^2$ is given by

$$\left|[\mathbf{y}_{l,\mathbf{U}}]_m\right|^2 \sim \frac{1}{2}\left(s_r + \sigma_v^2\right)\chi^2\left(2\right) \tag{62}$$

where $[\mathbf{y}_{l,\mathbf{U}}]_m$ is the m-th item of $\mathbf{y}_{l,\mathbf{U}}$, $\chi^2(2)$ represents a chi-square variable with 2 degrees of freedom. For ease of notation, the distribution of $\left|[\mathbf{y}_{l,\mathbf{U}}]_m\right|^2$ is denoted by X_m.

The moment-generating function (MGF) of (62) is

$$M_{X_m}(t) = \frac{1}{1 - \left(s_r + \sigma_v^2\right)t}. \tag{63}$$

Note that $X_{m|m=1,2,\ldots,M}$ are independent identically distributed (i.i.d.) random variables. Thus the MGF of z can be represented by

$$M_z(t) = \prod_{m=1}^{M} M_{X_m}\left(\frac{t}{M}\right) = \frac{1}{\left(1-\theta\left(s_r\right)t\right)^M} \tag{64}$$

where $\theta(s_r) = (s_r + \sigma_v^2)/M$.

The MGF of a gamma variable with shape k and scale θ is given by

$$M_{\texttt{gamma}}\left(t\right) = \left(1-\theta t\right)^{-k} \quad \text{for} \;\; t < \frac{1}{\theta}. \tag{65}$$

Obviously, for $t < 1/\theta(s_r)$, the MGF of z is the same as the MGF of gamma variable with $k = M$ and $\theta = \theta(s_r)$. It is well known that if two distributions have the same MGF, then they are identical at almost all points [24]. That is,

$$M_X\left(t\right) = M_Y\left(t\right) \;\rightarrow F_X\left(x\right) = F_Y\left(x\right). \tag{66}$$

Therefore, z follows a gamma distribution with $k = M$ and $\theta = \theta(s_r)$. Hence, the proof of Proposition 1 is concluded.

APPENDIX B
PROOF OF PROPOSITION 2

Suppose $\{X_1, X_2, \ldots, X_n\}$ is a sequence of i.i.d. random variables with $\mathbb{E}[X_i] = \mu$ and $\text{Var}[X_i] = \sigma^2$. According to the Lindeberg-Lévy CLT [26], as n approaches infinity, the random variable $\sqrt{n}\left(\frac{1}{n}\sum_{i=1}^{n} X_i - \mu\right)$ converges in distribution to a Gaussian variable $\mathcal{N}(0, \sigma^2)$, i.e.

$$\sqrt{n}\left(\frac{1}{n}\sum_{i=1}^{n} X_i - \mu\right) \;\xrightarrow{d}\; \mathcal{N}\left(0, \sigma^2\right). \tag{67}$$

The Gaussian distributions are closed under linear transformations. That is, if X is normally distributed with mean μ and variance σ^2, then a linear transform $aX + b$ (for some real numbers a and b) is also normally distributed [27]

$$aX + b \sim \mathcal{N}\left(a\mu + b,\, a^2\sigma^2\right). \tag{68}$$

Therefore, (67) changes to

$$\frac{1}{n}\sum_{i=1}^{n} X_i \;\xrightarrow{d}\; \mu + \frac{1}{\sqrt{n}}\mathcal{N}\left(0, \sigma^2\right) = \mathcal{N}\left(\mu, \frac{\sigma^2}{n}\right). \tag{69}$$

Due to the independence among channel realizations, the received signals at different antennas are mutually independent. Thus, the distribution of $[\mathbf{y}_{l,\mathbf{U}}]_m$ is

$$[\mathbf{y}_{l,\mathbf{U}}]_m \sim \mathcal{CN}\left(0, s_r + \sigma_v^2\right). \tag{70}$$

The decision metric is represented by

$$z = \frac{\|\mathbf{y}_{l,\mathbf{U}}\|_2^2}{M} = \frac{1}{M}\sum_{m=1}^{M}\left|[\mathbf{y}_{l,\mathbf{U}}]_m\right|^2. \tag{71}$$

Because $\left|[\mathbf{y}_{l,\mathbf{U}}]_m\right|^2$ follows i.i.d. chi-square distributions, then according to (69) we have

$$\frac{1}{M}\sum_{m=1}^{M}\left|[\mathbf{y}_{l,\mathbf{U}}]_m\right|^2 \xrightarrow{d} \mathcal{N}\left(\mathbb{E}\left[\left|[\mathbf{y}_{l,\mathbf{U}}]_m\right|^2\right], \frac{\text{Var}\left[\left|[\mathbf{y}_{l,\mathbf{U}}]_m\right|^2\right]}{M}\right) \tag{72}$$

where

$$\begin{aligned}\mathbb{E}\left[\left|[\mathbf{y}_{l,\mathbf{U}}]_m\right|^2\right] &= \mathbb{E}\left[\Re\left\{[\mathbf{y}_{l,\mathbf{U}}]_m\right\}^2\right] + \mathbb{E}\left[\Im\left\{[\mathbf{y}_{l,\mathbf{U}}]_m\right\}^2\right] = s_r + \sigma_v^2,\\ \text{Var}\left[\left|[\mathbf{y}_{l,\mathbf{U}}]_m\right|^2\right] &= \text{Var}\left[\Re\left\{[\mathbf{y}_{l,\mathbf{U}}]_m\right\}^2\right] + \text{Var}\left[\Im\left\{[\mathbf{y}_{l,\mathbf{U}}]_m\right\}^2\right] = \left(s_r + \sigma_v^2\right)^2.\end{aligned} \tag{73}$$

Thus, the proof of Lemma 2 is concluded.

APPENDIX C
PROOF OF PROPOSITION 3

If the sizes of users' constellations are different, the SER can be further optimized. For the isometric constellation, the following relationship can be derived

$$\frac{s_r - s_{r-1}}{2} = \Delta_{L,r} = \Delta_{R,r} = \frac{1}{(N_1 - 1)\prod_{u=2}^{U} N_u}. \tag{74}$$

Then, it can be observed that $(s_r - s_{r-1})/2$ is decided by the constellation size. On the other hand, the SER depends on $(s_r - s_{r-1})/2$. Thus, minimizing the SER can be transformed into maximizing (74), i.e.

$$\begin{aligned}\max_{\{\mathsf{N}\}} \quad & \frac{1}{(N_1 - 1)\prod_{u=2}^{U} N_u},\\ \text{s.t.} \quad & \mathsf{N} = \{N_1, N_2, \ldots, N_U\}.\end{aligned} \tag{75}$$

The cost function in (75) is shown as

$$\frac{1}{(N_1 - 1)\prod_{u=2}^{U} N_u} = \frac{1}{\prod_{u=1}^{U} N_u - \frac{\prod_{u=1}^{U} N_u}{N_1}}. \tag{76}$$

Since $\prod_{u=1}^{U} N_u$ is fixed, the value of (76) is only decided by N_1. Maximizing (76) equals to minimizing N_1. Therefore, the optimization can be solved by $N_1 = \min\{\mathsf{N}\}$. As a result, the size of the first constellation is the smallest among u users. Combined the results above, Proposition 3 is obtained.

APPENDIX D
PROOF OF THE PROBABILITY OF SYMBOL ERRORS IS AN INCREASING FUNCTION OF U

Here, we investigate the relationship between P_e and U, which is denoted by $f(U)$ in the following. The influence of noise is neglected, that is, $\sigma_v^2 \to 0$. Hence, the decision region is computed by $d_r = \frac{s_r + s_{r+1}}{2}$.

First, by defining $\omega = \prod_{u=1}^{U} N_u$, $f(U)$ is able to be written as

$$f\left(U\right) = \frac{1}{2\omega} \sum_{r=1}^{\omega} \left(\text{erfc}\left(\frac{\Delta_{L,r}}{\sqrt{2}\sigma\left(s_r\right)} \right) + \text{erfc}\left(\frac{\Delta_{R,r}}{\sqrt{2}\sigma\left(s_r\right)} \right) \right). \tag{77}$$

Then, according to $s_2 - s_1 = s_3 - s_2 = \cdots = s_{\prod_{u=1}^{U} N_u} - s_{\prod_{u=1}^{U} N_u - 1} = \theta$ in (43), $\frac{\Delta_{L,r}}{\sqrt{2}\sigma(s_r)}$ and $\frac{\Delta_{R,r}}{\sqrt{2}\sigma(s_r)}$ can be separately represented as

$$\begin{aligned} \frac{\Delta_{L,r}}{\sqrt{2}\sigma\left(s_r\right)} &= \sqrt{\frac{M}{2}} \frac{s_r - d_{r-1}}{s_r} = \sqrt{\frac{M}{2}} \frac{\theta}{2s_r}, \\ \frac{\Delta_{R,r}}{\sqrt{2}\sigma\left(s_r\right)} &= \sqrt{\frac{M}{2}} \frac{d_r - s_r}{s_r} = \sqrt{\frac{M}{2}} \frac{\theta}{2s_r}. \end{aligned} \tag{78}$$

Notice that for $s_1 = 0$, the following result is attainable

$$\text{erfc}\left(\frac{\Delta_{L,1}}{\sqrt{2}\sigma\left(s_1\right)} \right) + \text{erfc}\left(\frac{\Delta_{R,1}}{\sqrt{2}\sigma\left(s_1\right)} \right) = 0. \tag{79}$$

Because the joint constellation is isometric, it comes to $s_r = (r-1)\theta$. Then, (77) can be rewritten by

$$f\left(U\right) = \frac{1}{\omega} \sum_{r=2}^{\omega} \text{erfc}\left(\sqrt{\frac{M}{2}} \frac{1}{2\left(r-1\right)} \right). \tag{80}$$

Here, $g(r)$ is used to express $\text{erfc}\left(\sqrt{\frac{M}{2}}\frac{1}{2(r-1)}\right)$. Obviously, $g(r)$ is an increasing function of r. For the purpose of simplicity, all the users are assumed to utilized constellations with the same size N. Therefore, by comparing $f(U+1)$ and $f(U)$, one can get

$$\begin{aligned} \frac{f\left(U+1\right)}{f\left(U\right)} = \frac{1}{N} \frac{\sum_{r=2}^{N^{U+1}} g\left(r\right)}{\sum_{r=2}^{N^U} g\left(r\right)} &= \frac{1}{N} \left(1 + \frac{\sum_{r=N^U+1}^{N^{U+1}} g\left(r\right)}{\sum_{r=2}^{N^U} g\left(r\right)} \right) \\ &> \frac{1}{N} \left(1 + \frac{\left(N^{U+1} - N^U\right) g\left(N^U\right)}{\left(N^U - 1\right) g\left(N^U\right)} \right) > \frac{N^{U+1} - 1}{N^{U+1} - N} > 1. \end{aligned} \tag{81}$$

Since $f(U+1) > f(U)$, it is proved that error probability is an increasing function of U.

REFERENCES

[1] F. Rusek, D. Persson, B. K. Lau, E. G. Larsson, T. L. Marzetta, O. Edfors, and F. Tufvesson, "Scaling up MIMO: Opportunities and challenges with very large arrays," *IEEE Signal Process. Mag.*, vol. 30, no. 1, pp. 40–60, Jan. 2013.

[2] L. Lu, G. Y. Li, A. L. Swindlehurst, A. Ashikhmin, and R. Zhang, "An overview of massive MIMO: Benefits and challenges," *IEEE J. Sel. Topics Signal Process.*, vol. 8, no. 5, pp. 742–758, Apr. 2014.

[3] T. L. Marzetta, "Noncooperative cellular wireless with unlimited numbers of base station antennas," *IEEE Trans. Wireless Commun.*, vol. 9, no. 11, pp. 3590–3600, Oct. 2010.

[4] F. Boccardi, R. W. Heath, A. Lozano, T. L. Marzetta, and P. Popovski, "Five disruptive technology directions for 5G," *IEEE Commun. Mag.*, vol. 52, no. 2, pp. 74–80, Feb. 2014.

[5] S. Rangan, T. S. Rappaport, and E. Erkip, "Millimeter-wave cellular wireless networks: Potentials and challenges," *Proceedings of the IEEE*, vol. 102, no. 3, pp. 366–385, Feb. 2014.

[6] K. Witrisal, G. Leus, G. J. M. Janssen, M. Pausini, F. Troesch, T. Zasowski, and J. Romme, "Noncoherent ultra-wideband systems," *IEEE Signal Process. Mag.*, vol. 26, no. 4, pp. 48–66, Jul. 2009.

[7] H. Urkowitz, "Energy detection of unknown deterministic signals," *Proceedings of the IEEE*, vol. 55, no. 4, pp. 523–531, Apr. 2005.

[8] R. W. Heath, N. González-Prelcic, S. Rangan, W. Roh, and A. M. Sayeed, "An overview of signal processing techniques for millimeter wave MIMO systems," *IEEE J. Sel. Topics Signal Process.*, vol. 10, no. 3, pp. 436–453, Feb. 2017.

[9] S. Z. Li, J. K. Zhang, and X. M. Mu, "Noncoherent massive space-time block codes for uplink network communications," *IEEE Transactions on Vehicular Technology*, vol. 67, no. 6, pp. 5013–5027, Mar. 2018.

[10] F. Wang, Z. Tian, and B. M. Sadler, "Weighted energy detection for noncoherent ultra-wideband receiver design," *IEEE Trans. Wireless Commun.*, vol. 10, no. 2, pp. 710–720, Dec. 2011.

[11] M. Chowdhury, A. Manolakos, and A. Goldsmith, "Scaling laws for noncoherent energy-based communications in the SIMO MAC," *IEEE Trans. Inf. Theory*, vol. 62, no. 4, pp. 1980–1992, Feb. 2016.

[12] H. Q. Xie, W. Y. Xu, W. Xiang, K. Shao, and S. Xu, "Non-coherent massive SIMO systems in ISI channels: Constellation design and performance analysis," *arXiv preprint arXiv:1809.02946*, 2018.

[13] A. O. Martinez, E. De Carvalho, P. Popovski, and G. F. Pedersen, "Energy detection using very large antenna array receivers," in *2014 Asilomar Conf. on Signals, Systems and Computers*, 2014, pp. 1034–1038.

[14] A. Manolakos, M. Chowdhury, and A. Goldsmith, "Energy-based modulation for noncoherent massive SIMO systems," *IEEE Trans. Wireless Commun.*, vol. 15, no. 11, pp. 7831–7846, Sep. 2015.

[15] L. Jing, E. D. Carvalho, P. Popovski, and Á. O. Martnez, "Design and performance analysis of noncoherent detection systems with massive receiver arrays," *IEEE Trans. Signal Process.*, vol. 64, no. 19, pp. 5000–5010, Jul. 2016.

[16] L. Jing, Z. Utkovski, E. D. Carvalho, and P. Popovski, "Performance limits of energy detection systems with massive receiver arrays," in *IEEE International Workshop on Computational Advances in Multi-Sensor Adaptive Processing*, 2016, pp. 205–208.

[17] L. S. Jing and E. D. Carvalho, "Energy detection in ISI channels using large-scale receiver arrays," in *IEEE International Conference on Acoustics, Speech and Signal Processing*, 2016, pp. 3431–3435.

[18] M. Chowdhury, A. Manolakos, and A. Goldsmith, "Multiplexing and diversity gains in noncoherent massive MIMO systems," *IEEE Trans. Wireless Commun.*, vol. 16, no. 1, pp. 265–277, Oct. 2017.

[19] M. Hammouda, S. Akin, and J. Peissig, "Performance analysis of energy-detection-based massive SIMO," in *IEEE International Black Sea Conference on Communications and Networking*, 2015, pp. 152–156.

[20] L. L. Dai, B. C. Wang, Y. F. Yuan, S. F. Han, C. lin I, and Z. C. Wang, "Non-orthogonal multiple access for 5G: Solutions, challenges, opportunities, and future research trends," *IEEE Communications Magazine*, vol. 53, no. 9, pp. 74–81, Sep. 2015.

[21] M. Sadeghi, E. Bjornson, E. G. Larsson, C. Yuen, and T. L. Marzetta, "Max-min fair transmit precoding for multi-group multicasting in massive MIMO," *IEEE Transactions on Wireless Communications*, vol. 17, no. 2, pp. 1358–1373, Dec. 2018.

[22] A. J. Viterbi, *CDMA: Principles of spread spectrum communication*. MA: Addison-Wesley, 1995.

[23] J. S. Rosenthal, *A first look at rigorous probability theory*. World Scientific, 2000.

[24] G. Grimmett and D. Welsh, *Probability*. Clarendon Press, 1986.

[25] Y. Y. Zhang, J. K. Zhang, and H. Y. Yu, "Physically securing energy-based massive MIMO MAC via joint alignment of multi-user constellations and artificial noise," *IEEE J. Sel. Areas Commun.*, vol. 36, no. 4, pp. 829–844, Apr. 2018.

[26] I. Barany and V. H. Vu, "Central limit theorems for gaussian polytopes," *Annals of Probability*, vol. 35, no. 4, pp. 1593–1621, 2007.

[27] Wikipedia, "Operations on normal deviates," https://en.wikipedia.org/wiki/Normal_distribution#Operations_on_normal_deviates.